Journal of
NANOSTRUCTURES
JNS
NANOSTRUCTURES
JNS.kashanu.ac.ir

Selective Magnetic Removal of Pb(II) from Aqueous Solution by Porphyrin Linked-Magnetic Nanoparticles

T. Poursaberi, H. Ghanbarnejad*, V. Akbar

Research institute of petroleum industry, P.O. Box 14665-137, Tehran, Iran

Article history:
Received 3/12/2012
Accepted 14/2/2013
Published online 1/3/2013

Keywords:
Magnetic nanoparticles
Surface modification
Lead removal
Porphyrins
Atropisomers

**Corresponding author:*
E-mail address:
ghanbarnejadh@ripi.ir
Phone: 98 912 5195058
Fax: +98 21 44739537

Abstract

The discharge of lead containing effluents into the environment and water bodies is harmful for the human, animals, aquatic flora and fauna. Herein, a novel surface engineered magnetic nanoparticle for removing Pb^{2+} ions was studied. After surface modification of the magnetite by 3-amino-propyltriethoxysilane (APTES) magnetic nanoparticles with covalently linked porphyrins were synthesized. Two atropisomers of *meso*-tetrakis(2-carboxy-4-nonylphenyl) porphyrin (TCNP) were tested to analyze the atropisomeric effect on lead uptake. For characterize the synthesized nanosorbents methods like: Transform Infrared Spectroscopy, X-ray diffraction, Transmission Electron Microscopy and Thermo-Gravimetric Analysis were used. The effects of pH, contact time, sorbent dosage and some co-existing cations were investigated. Regeneration of lead adsorbed material could be possible and the modified magnetic nanoparticles exhibited good reusability. The use of such a system can provide fast and efficient removal of the lead ion by using an external magnetic field. The competitive adsorption tests showed good adsorption selectivity for lead ion.

1. Introduction

The discharge of lead containing effluents such as the wastewater from printed circuit board factories, electronics assembly plants and battery recycling plants [1-3] into the environment and water bodies cause serious public concerns. It is known that lead is harmful for human and animals health and causes blood enzyme changes, hyperactivity and neurological disorders [4]. Under specific conditions lead promotes protein and DNA synthesis and stimulates cell replication. Pb^{2+} ion has high affinity toward thio- containing enzymes and prohibits the biosynthesis of the hem units, as a result permeability of kidney, liver and brain cells are affected [5]. Even relatively low concentrations of Lead endanger the aquatic flora

and fauna [1–3]. Currently the EPA standard for drinking water is 0.05 mg/l, but a level of 0.02 mg/l is under review [6]. Therefore efficient technologies development for lead abatement is necessary.

Lots of separation methods such as ion exchange process [7, 8], reverse osmosis [9], electrolytic methods [10], adsorption [11] and precipitation [12] have been used to remove metal ions from wastewater. Amongst these technologies adsorption is widely used and satisfactory result has provided [13-16].

Nanostructured materials often come with unique properties which make them applicable for a variety of novel applications [17, 18]. But their main drawback is the complex separation process due to their small size. Causes of easy separation by applying a magnetic field, magnetic nanoparticles have been the focus of much research recently. Since these naked magnetic materials are susceptible to air oxidation and also form large aggregates by interacting with each other, [19] it is often necessary to coat the surface of the pristine magnetic nanoparticles, e.g. by 3-aminopropyl-triethoxysilane [20, 21]. In addition by tailoring the surface of these modified nanoparticles; one can provide active surfaces which induce selective adsorption of target ions [22-24]. So core-shell-shell type magnetic nanoparticles could achieve which can be used as an attractive adsorbent for marked ions from industrial wastes or natural water streams [25, 26]. Nonfunctional iron oxide has been previously used as metal adsorber [27-30], but control of metal selectivity was limited, and the interactions between the iron oxide and metal were often irreversible [30, 31].

The prophyrins attracted much attention as soft heavy metals ionophores due to metal binding properties, rapid exchange kinetics, and water insolubility [32-35]. Their characteristics provide geometric control of host-guest complex; modulation of their lipophilicity; producing significant selectivity, sensitivity and stability toward a specific ion. As a result they have been successfully applied for the construction of different cation selective electrodes such as Ni^{2+}, Co^{2+}, Zn^{2+} and so on [36-38]. Lee et.al showed that among the *meso*-Tetrakis(2-hydroxy-1-naphthyl)porphyrin atropisomers, (α,α,α,α)-THNP displays a good and selective response to Pb^{2+} [39]. The objective of the present work was to investigate the role and the efficiency of two atropisomers of *meso*- tetrakis(2-carboxyl-4-nonylphenyl) porphyrin (TCNP), including (α,α,α,α) and (α,β,α,β)-TCNP, as functionalized groups of magnetic nanosorbent in the adsorption of lead ions from aqueous solution. The presence of the four (*o*-carboxy) substituents on the nonylphenyl group connected to *meso* positions of porphyrin facilitates the functionalization of amino-silane coated magnetite through amide bond formation. The effect of TCNP atropisomers along with other affecting parameters such as pH, contact time, nanosorbent dosage and some co-existing cations on lead removal efficiency was investigated. The preparation of different functionalized magnetic nanoparticles has been reported in the literature [40-45]; but porphyrin grafted-magnetic adsorbent which possesses selective targeting has not been reported and is the topic of the present study.

2. Experimental

2. 1. Materials

Ferric chloride hexahydrate, ferrous chloride tetrahydrate, APTES, dichloromethane (DCM), *N*,*N*-dimethylformamide (DMF), dicyclohexyl

carbodiimide (DCHC), methanol, ammonia, nitrate salts of indicated cations were all analytical grade from Merck Chemical Co. The atropisomers of TCNP (Fig.1) were prepared according to the procedure described in literatures [46, 47].

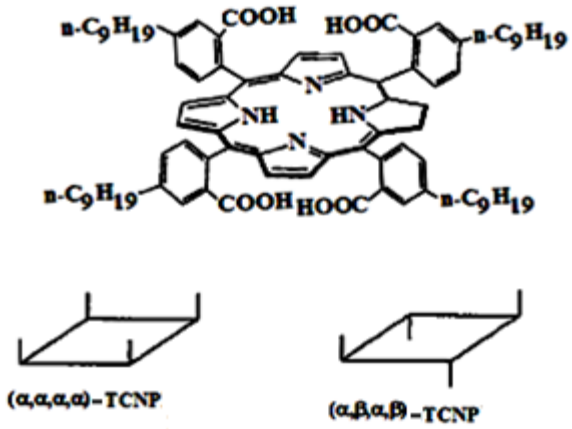

Fig. 1. Schematic representation of the porphyrins used in this work.

2. 2. Equipments

The morphology and dimension of the Fe_3O_4/APTES/TCNP were obtained from transmission electron microscopy (TEM) using a Zeiss 900 TEM at a voltage of 80 kV. The phase purity was characterized by X-ray powder diffraction (XRD) (PW-1840 diffractometer from Philips Co.) using Cu-K_α radiation (λ=1.54178 Å). The metallic ions were determined using a graphite furnace atomic absorption spectrometer (GFAAS, Thermo Elemental, Solar GF 95, and UK). pH measurements were performed with a Metrohm 691 pH meter. FTIR spectra were obtained using a Vertex 70 FT-IR spectrophotometer from Bruker Co to identify the functional groups and chemical bonding of the coated materials. TGA were performed with a Mettler Toledo TGA/SDTA 851 instrument. Samples were heated under static air atmosphere from ambient to 1000 °C at a rate of 10°C min^{-1}.

2. 3. Sorbent preparation

Synthesis of the porphyrin-grafted Fe_3O_4 nanoparticles was carried out in three stages:

(a) Fe_3O_4 magnetic particles were prepared according to maity et. al procedure [48].

(b) To obtain modified magnetite nanoparticles, the surface of Fe_3O_4 should be coated through silanization reaction with APTES. Therefore through sonication a homogeneous suspension has been made by mixing 3.7 g of magnetite with 40 mL of toluene, followed by the addition of 19.5 mmol APTES. The reaction mixture was kept at room temperature for 5 h under nitrogen atmosphere with vigorous mechanical stirring. Then obtained APTES-immobilized magnetite magnetically collected, washed with ethanol and de-ionized water and vacuum dried at 70 °C.

(c) In order to functionalize the modified nanoparticles, Fe_3O_4/APTES and DCHC were suspended in DMF under nitrogen. TCNP was dissolved in DMF and added dropwise to the suspension. The mixture was refluxed at 140 °C for 8 h under high flux of nitrogen [49] and Fe_3O_4/APTES/TCNP nanoparticles were magnetically isolated. To eliminate porphyrins that are electrostatically bonded to Fe_3O_4/APTES, they were washed with DMF, CH_2Cl_2 and methanol. A scheme of the magnetite surface modification process is shown in Fig. 2.

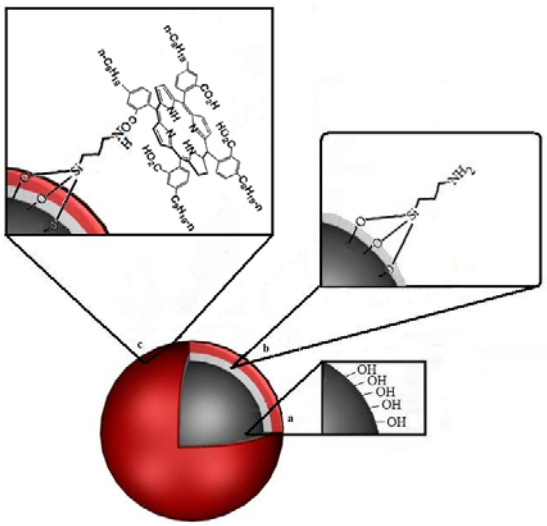

Fig. 2. Chemical functionalization magnetite (a) surfaces using APTES(b) followed by porphyrin insertion(c).

2. 4. Sorption procedure

Lead adsorption by Fe_3O_4/APTES/TCNP has been studied in batch experiments. A known amount of sorbent was mixed with 10 ml of 20 mg/L aqueous lead solution and then a magnetic field of 100Hz and 1200 Oe applied to rotate the nanosorbents over a period of time. The aqueous phase was magnetically decanted and lead concentration was calculated according to Eq. (1):

$$\text{Lead removal efficiency}(\%) = \left[\frac{C_0 - C_r}{C_0}\right] \times 100 \quad (1)$$

Where C_o and C_r are the initial and final concentrations of the lead ion before and after the sorption, respectively.

3. Results and discussion

3. 1. Characterization

The identity and the phase purity of the synthesized nanosorbent were checked by XRD (Fig.3). The Joint Committee on Powder Diffraction Standards (JCPDS) reference pattern of magnetite (No. 19-629) was used for comparison. As can be seen, the XRD pattern of functionalized magnetite nanoparticles was in good agreement with that of the standard Fe_3O_4 structure, indicating that the APTES coating and porphyrin grafting did not result in the phase change of Fe_3O_4.

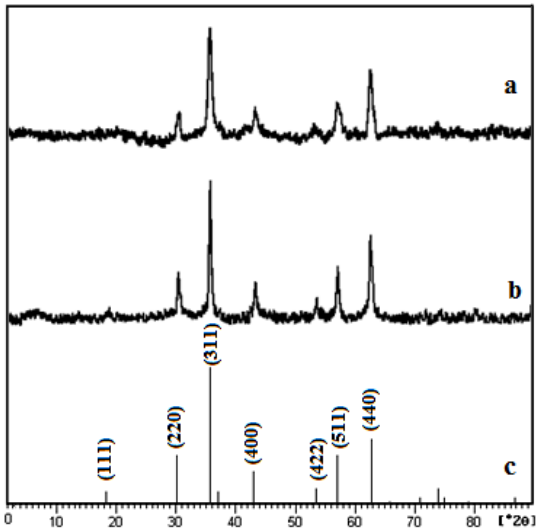

Fig. 3. XRD patterns of (a) Fe_3O_4/APTES/(α,α,α,α)-TCNP, (b) Fe_3O_4/APTES/(α,β,α,β)-TCNP nanosorbents and (c) standard magnetite pattern (JCPDS no. 19-0629).

The introduction of TCNP into the magnetite nanoparticles was evident from TEM results. The dark nano-Fe_3O_4 cores surrounded by a grey shell could be observed in Fig. 4. Moreover, the bare Fe_3O_4 nanoparticles had a mean diameter of about 10 nm, much smaller than the functionalized ones (53 nm (a) and 48 nm (b)).

To warrant the successful functionalization of Fe_3O_4 with TCNP, we employed IR to give detailed investigations of the obtained sorbent (Fig. 5). The strong bond at 580cm^{-1} corresponds to Fe-O vibrations of the magnetite core. The bands around 1030 and 1115 cm^{-1} belong to the Si-O–H and Si–O–Si groups and verified the introduction of APTES to the surface of Fe_3O_4 nanoparticles. The covalent anchoring of aminopropylsilane groups can be proved by absorption bands at 2930

and 2862 cm^{-1} assigned to stretching vibration of C–H bond of the propyl amine group. The two bands at 3445 and 1640 cm^{-1} can be ascribed to the N–H stretching vibration and NH_2 bending mode of free NH_2 groups, respectively. The FT-IR spectrum revealed a peak at 1689 cm^{-1} relating to the amide group stretching band, which proves that the TCNP can be covalently attached to the amine groups of APTES through the formation of a stable amide bond.

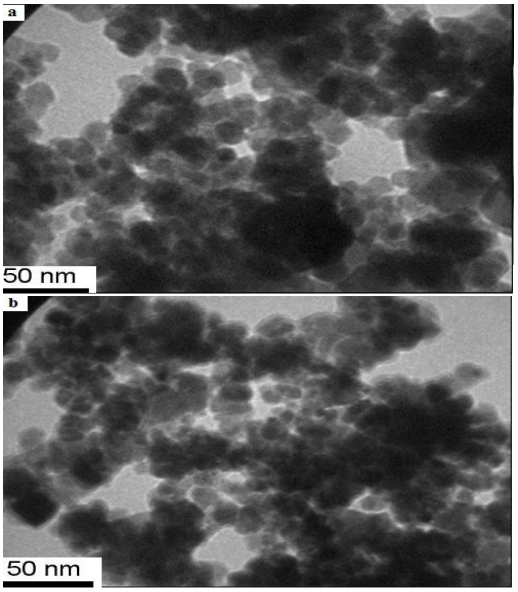

Fig. 4. TEM images of (a) Fe_3O_4/APTES/(α,α,α,α)-TCNP and (b) Fe_3O_4/APTES/(α,β,α,β)-TCNP nanosorbents.

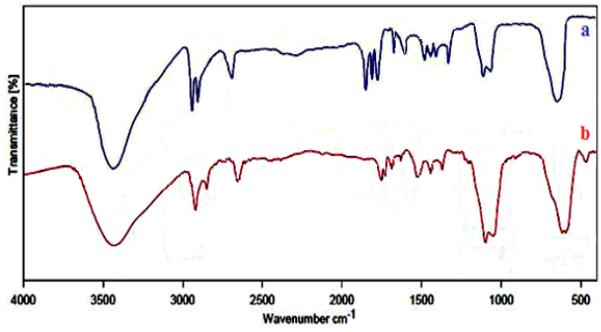

Fig. 5. FTIR spectra of (a) Fe_3O_4/APTES/(α,α,α,α)-TCNP and (b) Fe_3O_4/APTES/ (α,β,α,β)-TCNP nanosorbents.

3.1.3. TGA analysis

The thermal stability of the synthesized nanosorbent was investigated and the TG curve of the Fe_3O_4/APTES/TCNP is shown in Fig. 6. As can be seen three stages of weight loss are detected: the first weight loss could be explained by the evaporation of the adsorbed solvent attached to the particle surfaces. The second weight-loss stage might result from loss of the APTES layer [50].The third weight-loss stage may result from the decomposition of porphyrins [51].

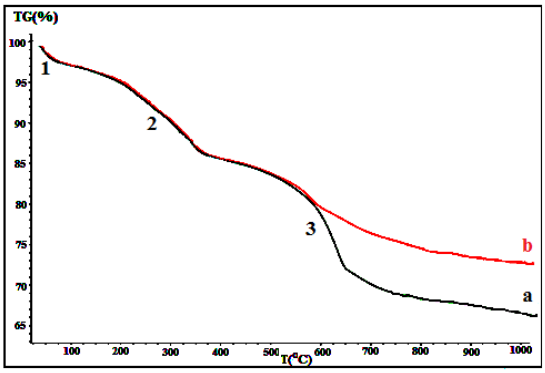

Fig. 6. TGA analysis of (a) Fe_3O_4/APTES/(α,α,α,α)-TCNP and (b) Fe_3O_4/APTES/ (α,β,α,β)-TCNP nanosorbents.

These data showed that coating and modification of Fe_3O_4 nanoparticles with TCNP has been performed and they have been bonded to each other chemically. This is an important result in this work to attach the porphyrin modifier onto the magnetic nanoparticles chemically instead of physical adsorption.

To obtain more information about the optimized structures of (α,α,α,α)-TCNP and (α,β,α,β)-TCNP upon complexation to the lead ions, the molecular structures of the free ligands and their complexes with Pb^{2+} were built with the Hyperchem program (Fig.7) [52]. It is interesting to note that the corresponding ΔE values calculated

by PM3 (Parameterized Model 3) semi-empirical calculations [53] for the resulting lead complexes, i.e., -157.593 kcal mol^{-1} for Pb^{2+}-(α,α,α,α)-TCNP and -140.408 kcal mol^{-1} for Pb^{2+}-(α,β,α,β)-TCNP, revealed that the (α,α,α,α)-TCNP complex of Pb^{2+} is more stable than the other adduct which was demonstrated in practice.

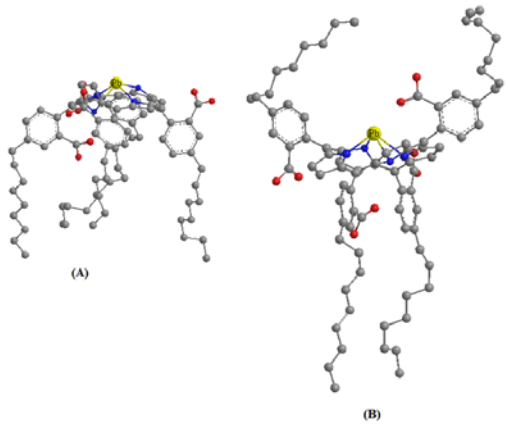

Fig. 7. Computer simulation representing the structure of the complexes of (α,α,α,α)-TCNP (A) and (α,β,α,β)-TCNP (B) with lead ion. Nitrogen atoms are in blue, oxygen in red, carbon in black. The hydrogen atoms are not represented.

3. 2. Adsorption experiments

Adsorption experiments were carried out in two steps: optimization of the main factors affecting the adsorption namely, pH of the solution, contact time, and sorbent dosage, and removal studies under optimal conditions.

Since pH played a key role in the adsorption process, the performance of the sorbent was studied in the pH range of 2.0–8.0 (Fig. 8). The sorption of lead initially increased with pH and a plateau occurred at pH 6 onwards. As presented in Fig. 8, under acidic pH conditions, the sorbents have lower adsorption tendencies. This was expectable as at lower pH the chelation sites on TCNP were occupied with H^+ and they were released at higher pH and form the desired chelation wit Pb^{2+}. The K_{sp} value for $Pb(OH)_2$ at 20 ^oC is 1.2×10^{-15}. The concentration used was 20 $mg1^{-1}$, so the pH after which the hydroxide of Pb(II) begin to produce was about 8.5. Therefore the adsorption studies at more alkaline solutions (pH >8) were not carried out. For subsequent experiments pH 6 was selected.

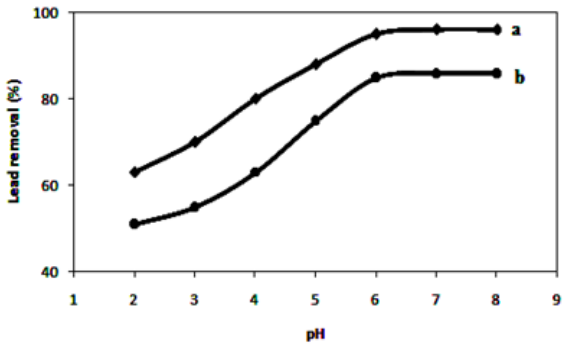

Fig. 8. The pH influence on the removal efficiency of lead; (a) Fe_3O_4/APTES/(α,α,α,α)-TCNP and (b) Fe_3O_4/APTES/ (α,β,α,β)-TCNP nanosorbents.

As the magnetic nanoparticles can easily rotate under the changing magnetic field, for larger volumes or more viscous liquids, it might work better to use an AC magnetic field to stir the nanosorbent instead of traditional mechanical stirring of the solution. So it could be a promising technology in treatment of large volumes of wastewater. The time dependant of lead removal from aqueous solutions was monitored for 90 min (Fig.9). It could be seen that the maximum lead removal was obtained within the first 20 min, then gradually reached equilibrium in 60 min and no significant change was observed in the following 30 min.

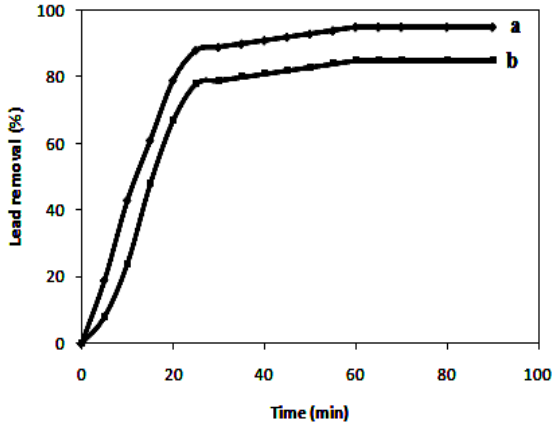

Fig. 9. Effect of contact time on the adsorption of lead by (a) Fe_3O_4/APTES/(α,α,α,α)-TCNP and (b) Fe3O4/APTES/ (α,β,α,β)-TCNP nanosorbents.

To find the optimum amount of nanosorbents which can remove lead ions from aqueous solution, a batch-mode sorption study was performed using various amounts (25–150 mg) of Fe_3O_4/APTES/TCNP nanosorbents. The lead removal efficiencies as a function of nanosorbents dosage are presented in Fig.10. It is evident that the percent of lead removal increased with the increase of the sorbent dosage which is due to the fact that a greater amount of sorbent implies a greater amount of available binding sites. As seen in Fig.10, the percent removal reached steady state value after 75 mg/L of Fe_3O_4/APTES/TCNP nanoadsorbents.

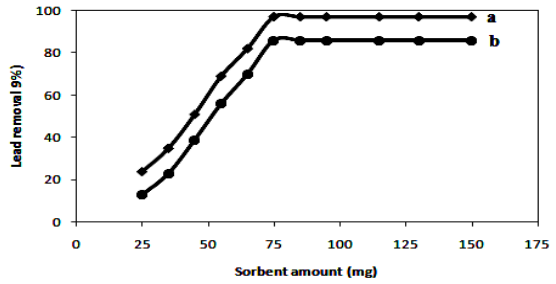

Fig. 10. Effect of nanosorbents dosage on the on lead removal; (a) Fe_3O_4/APTES/(α,α,α,α)-TCNP and (b) Fe_3O_4/APTES/ (α,β,α,β)-TCNP nanosorbents.

To check the reversibility of lead adsorption reaction with Fe_3O_4/APTES/TCNP nanosorbents, regeneration of the lead-loaded nanosorbent was contacted with various concentrations of HCl (5-20 mM) as eluent solution and then the percentage of desorption was calculated. The maximum recovery of lead (95.7%) was achieved with 10 mM HCl.

After the first regeneration, the adsorption studies were repeated. The nanosorbents were again regenerated and subjected to further use. After four adsorption–desorption cycles, the efficiency of nanosorbent for the lead removal was not significantly reduced (not more than 5%) but at fifth run a 10% decrease in its performance was observed; therefore the desorption limit for lead was four cycles. It could be concluded that the chemical bonding between TCNP and magnetic nanoparticles plays the major role in retaining the capacity of the Fe_3O_4/APTES/TCNP nanosorbents.

In order to evaluate the performance of the synthesized nanomagnet for lead removal, extraction was carried out under optimal conditions. The deionized water was spiked with lead ion to make a 20 mgL^{-1} solution. The batch adsorption experiment was carried out on 10 mL of this spiked sample under optimal conditions; i.e. contact time: 20 minutes, pH 6 and sorbent dosage: 75 mg. It was found that the lead content after treatment with (α,α,α,α)-TCNP and (α,β,α,β)-TCNP -contained nanosorbents decreased from 20.0 mgL^{-1} to 0.6 mgL^{-1} and 2.8 mgL^{-1} respectively. As it is clear, the nanosorbent contains (α,β,α,β)-TCNP resulted in a diminished removal efficiency (86%) with respect to the (α,α,α,α)-TCNP-contained nanosorbent (97%) which is in support of the theoretical calculations (Sec.3.1.4). The above result demonstrates that

(α,α,α,α)-TCNP, having the same oriented direction of four *o*-carboxy substituents on the nonylphenyl groups, behaves as a much more suitable ligand than the other for Pb^{2+} ion. This is most probably because of the effect of the ligand rigidity due to the same oriented direction and the hindered rotation of the nonylphenyl groups in (α,α,α,α)-TCNP.

The lead removal from real samples is dependent upon the presence of other cations which could compete for the binding sites with lead and caused lower lead uptake. Therefore the bi-cation adsorption of nanosorbent was examined in the presence of co-cations viz., alkaline and alkaline-earth ions, as well as some transition and heavy metals ions (Fig.11). These experiments were performed with a fixed lead concentration of 20 mgL^{-1} while the concentration of each coexisting cation varied within two orders of magnitude. The tolerance limit was defined as the amount of the foreign cation causing a change of ±5% in the lead removal efficiency. As seen from Fig.11, the removal percentage of lead were remained within the tolerance limit in the presence of the ten folded concentration of the Zn^{2+} and Ni^{2+}, fifty folded of Cu^{2+},Co^{2+}, Hg^{2+} and one hundred folded of Na^{+}, K^{+}, Mg^{2+} and Ca^{2+} concentrations. Therefore these cations would not significantly disturb the functioning of the Pb^{2+} nanosorbent.

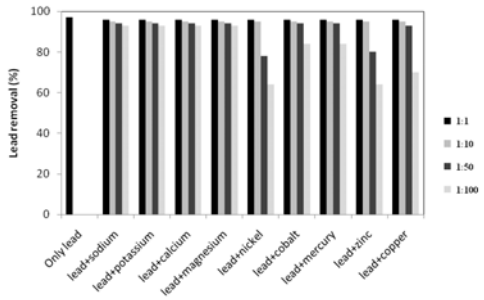

Fig. 11. Effect of co-existing anions on lead removal by Fe_3O_4/APTES/(α,α,α,α)-TCNP nanosorbents.

In order to check the applicability of proposed nanosorbent for lead removal from actual field conditions,(α,α,α,α)-TCNP-contained nanosorbent was tested with a groundwater sample. In the used groundwater sample the lead concentration was reduced from 3 to 0.16 mg l^{-1}, so the percentage of lead ions removal was 94.5%. As it is obvious the lead removal efficiency of real sample is lower than those of the spiked water, as the groundwater contains more cations which decrease the lead removal ability of nanosorbent.

4. Conclusion

We have presented a new nanosorbent which demonstrates the feasibility of lead removal from water media. The magnetite cores were prepared by coprecipitation of Fe^{2+} and Fe^{3+} with NH_4OH, followed by surface modification with APTES and an atropisomer of TCNP. FTIR analysis shows that porphyrin molecules have been incorporated onto the surface of the magnetite nanoparticles by CON chemical bonds. The proposed nanosorbent has good selectivity over monovalent and divalent cations. The result indicates that the geometry of the atropisomers of TCNP should be a significant factor for determining a selectivity toward other and the good sensitivity and highest selectivity towards lead ion are attributed to the strong complexation of lead ion to (α,α,α,α)-TCNP atropisomer which has the same oriented direction of four *o*-carboxy substituents on the nonylphenyl groups. The proposed nanosorbent is a good reusable adsorbent in removal of lead ion with the ease of separation by an external magnetic field and works well in actual field conditions.

References

[1] R.. Jalali, H. Ghafourian, Y. Asef, S.J. Davarpanah, S.J. Sepehr, Hazard. Mater. 92 (2002) 253.

[2] V. K. Gupta, M. Gupta, S. Sharma, Water Res. 35(5) (2001) 1125.

[3] K. Conrad, H. C. B. Hansen, Bioresour. Technol. 98(1) (2007) 89.

[4] E. M. Erfurth, L. Gerhardsson, A. Nilsson, L. Rylander, A. Schutz, S. Skerfving, Arch. Environ. Health 56 (2001) 449.

[5] A. I. Okoye, P. M. Ejikeme, O. D. Onukwuli, International Journal of Environment Science and Technology, 7(4) (2010) 793.

[6] A. Groffman, S. Peterson, D. Brookins, Water Environ. Technol. 5 (1992) 54.

[7] A. Smara, R. Delimi, E. Chainet, J. Sandeaux, Sep. Purif. Technol. 57 (2007) 103.

[8] L. Metcalf, H. P. Eddy, Wastewater Engineering Treatment and Reuse, 4th ed., McGraw Hill, New York, 2003.

[9] B. A. Winfield, Water Res. 13 (1979) 561.

[10] W. R. Peters, E. T. White, Y. K. Carole, S. J. Shedroll, Water Pollut. Control Fed. 58 (1986) 481.

[11] J. Patterson, Industrial Wastewater Treatment Technology, 2nd ed., Butter worth Publisher, Boston, 1985.

[12] J. R. Anderson, C. O. Weiss, Method for precipitation of heavy metal sulphides, USA, Patent, 3740331; June, 1973.

[13] N. N. J. Nassar, Haz. Mat. 184 (2010) 538.

[14] A. R. Mahdavian, M. Mirrahimi, Chemical Engineering Journal 159 (2010) 264.

[15] A. Uheida, G. Salazar-Alvarez, E.Björkman, Z. Yu, M. Muhammed, Journal of Colloid and Interface Science 298 (2006) 501.

[16] J. H. Jang, H. B. Lim, Microchemical Journal 94 (2010) 148.

[17] R. W. Siegel, E. Hu, M. C. Roco, Nanostructure Science and Technology, A Worldwide Study, WTEC, Loyola College Kluwer Academic, Baltimore, MD, 1999.

[18] C. Medina, M. J. Santos-Martinez, A. Radomski, O. I. Corrigan, M. W. Br. J. Radomski, Pharmacol. 150 (2007) 552.

[19] W.Wu, Q. He, C. Jiang, Nanoscale Res. Lett. 3 (2008) 397.

[20] E. A. Smith, W. Chen, Langmuir 24 (2008) 12405.

[21] K. Herve, L. Douziech-Eyrolles, E. Munnier, S. Cohen-Jonathan, M. Souce, H. Marchais, P. Limelette, F. Warmont, M. L. Saboungi, P. Dubois, I. Chourpa, Nanotechnology (2008) 19:465608.

[22] J. L. Lyon, D. A. Fleming, M. B. Stone, P. Schiffer, M. E. Williams, Nano. Lett. 4 (2004) 719.

[23] C. Xu, K. Xu, H. Gu, R. Zheng, H. Liu, X. Zhang, Z. Guo, B. J. Xu, Am. Chem. Soc. 126 (2004) 9938.

[24] A. Ulman, Chem. Rev. 96 (1996) 1533.

[25] C. Z. J. Huang, Sep. Sci. 31 (2008) 760.

[26] A. F. Ngomsik, A. Bee, M. Draye, G. Cote, V. C. R. Cabuil, Chimie 8 (2005) 963.

[27] H. Tamura, R. J. Furrichi, Colloid Interf. Sci. 195 (1997) 241.

[28] S. E. Ziemniak, L. M. Anovitz, M. L. Machesky, P. Benezeth, D. A. Palmer, Solubility and surface adsorption characteristics of metal oxides, in: D.A. Palmer, R. Fernandez-Prini, A.H. Harvey (Eds.), Aqueous Systems at Elevated Temperatures and Pressures, Elsevier, London, (2004) 493.

[29] R. M. McKenzie, Aust. J. Soil Res. 18 (1980) 61.

[30] D. A. Clifford, G. L. Ghurye, Metal-oxide adsorption, ion exchange, and coagulation-microfiltration for arsenic removal from water, in: W.T. Frankenberger Jr. (Ed.), Environmental Chemistry of Arsenic, Marcel Dekker, Inc., New York, (2002) 217.

[31] C. T. Yavuz, J. T. Mayo, W. W. Yu, A. Prakash, J. C. Falkner, S. Yean, L. Cong, H. J. Shipley, A. Kan, M. Tomson, D. Natelson, V. L. Colvin, Science 314 (2006) 964.

[32] M. Biesaga, K. Pyrzynska, M. Trojanowicz, Talanta 44 (1994) 881.

[33] M. N. Hughes, The Inorganic Chemistry of Biological Processes, Wiley, New York, 1981.

[34] J. W. Owens, O. Connor, Coord. Chem. Rev. 84 (1998) 1.

[35] S. L. Edwards, T. L. J. Poulos, Biol. Chem. 265 (1990) 2588.

[36] V. K. Gupta, A. K. Jain, L. P. Singh, U. Khurana, Anal. Chim. Acta 355 (1997) 33.

[37] A. K. Jain, V. K. Gupta, L. P. Singh, U. Khurana, Analyst 122 (1997) 122, 583.

[38] A. R. Fakhari, M. Shamsipur, Kh. Ghanbari, Anal. Chim. Acta 460 (2002) 177.

[39] H. K. Lee, K. Song, H. R. Seo, Y. Choi, S. Jeon, Sensors and Actuators B 99 (2004) 323.

[40] X. L. Zhao, Y. L. Shi, Y. Q. Cai, S. F. Mou, Environ. Sci. Technol. 1139 (2008) 178.

[41] W. Yantasee, C. L. Warner, T. Sangvanich, R. S. Addleman, T. G. Carter, R. J. Wiacek, G. E. Fryxell, C. Timchalk, M. G. Warner, Environ. Sci. Technol. 41 (2007) 5114.

[42] L. Cumbal, A. Sengupta, Environ. Sci. Technol. 39 (2005) 6508.

[43] X. L. Zhao, Y. L. Shi, T. Wang, Y. Q. Cai, G. B Jiang, J. Chromatogr. A 1188 (2008) 140.

[44] S. Y. Mak, D. H. Chen, Dyes Pigments 61 (2004) 93.

[45] L. M. Blaney, S. Cinar, A. K. Sen Gupta, Water Res. 41 (2007) 1603.

[46] T. Hayashi, T. Miyahara, N. Koide, Y. Kato, H. Masuda, H. Ogosh, J. Am. Chem. Soc. 119 (1997) 7281.

[47] Y. Kurodaa, A. Kawashimaa, T. Uraia, H. Ogoshia, Tetrahedron Letters 36 (1995) 8449.

[48] D. Maity, D. C. Agrawal, J. Magn. Magn. Mater. 308 (2007) 46.

[49] R. B. S. Merrifield, J. Am. Chem. Soc. 85 (1963) 2149.

[50] M. Epinosa, S. Pacheco, R. Rodriguez, Journal of non-crystalin solids 353 (2007) 2573.

[51] J. H. Cai, J. W. Huang, P. Zhao, Y. J. Ye, H. C. Yu, L.N. Ji, J. Sol-Gel Sci. Technol. 50 (2009) 430.

[52] Hyperchem, Release 7.0, Hypercube, Inc., Gainesville, 2002.

[53] J. J. P. Stewart, J. Comput. Chem. 10(1989) 209.